CLEO-CONF 05-5
LP2005-428

Improved Measurement of $\mathcal{B}(D^+ \to \mu^+\nu)$ and the Pseudoscalar Decay Constant f_{D^+}*

G. Bonvicini,[1] D. Cinabro,[1] M. Dubrovin,[1] R. A. Briere,[2] G. P. Chen,[2] J. Chen,[2] T. Ferguson,[2] G. Tatishvili,[2] H. Vogel,[2] M. E. Watkins,[2] J. L. Rosner,[3] N. E. Adam,[4] J. P. Alexander,[4] K. Berkelman,[4] D. G. Cassel,[4] V. Crede,[4] J. E. Duboscq,[4] K. M. Ecklund,[4] R. Ehrlich,[4] L. Fields,[4] L. Gibbons,[4] B. Gittelman,[4] R. Gray,[4] S. W. Gray,[4] D. L. Hartill,[4] B. K. Heltsley,[4] D. Hertz,[4] C. D. Jones,[4] J. Kandaswamy,[4] D. L. Kreinick,[4] V. E. Kuznetsov,[4] H. Mahlke-Krüger,[4] T. O. Meyer,[4] P. U. E. Onyisi,[4] J. R. Patterson,[4] D. Peterson,[4] E. A. Phillips,[4] J. Pivarski,[4] D. Riley,[4] A. Ryd,[4] A. J. Sadoff,[4] H. Schwarthoff,[4] X. Shi,[4] M. R. Shepherd,[4] S. Stroiney,[4] W. M. Sun,[4] D. Urner,[4] T. Wilksen,[4] K. M. Weaver,[4] M. Weinberger,[4] S. B. Athar,[5] P. Avery,[5] L. Breva-Newell,[5] R. Patel,[5] V. Potlia,[5] H. Stoeck,[5] J. Yelton,[5] P. Rubin,[6] C. Cawlfield,[7] B. I. Eisenstein,[7] G. D. Gollin,[7] I. Karliner,[7] D. Kim,[7] N. Lowrey,[7] P. Naik,[7] C. Sedlack,[7] M. Selen,[7] E. J. White,[7] J. Williams,[7] J. Wiss,[7] K. W. Edwards,[8] D. Besson,[9] T. K. Pedlar,[10] D. Cronin-Hennessy,[11] K. Y. Gao,[11] D. T. Gong,[11] J. Hietala,[11] Y. Kubota,[11] T. Klein,[11] B. W. Lang,[11] S. Z. Li,[11] R. Poling,[11] A. W. Scott,[11] A. Smith,[11] S. Dobbs,[12] Z. Metreveli,[12] K. K. Seth,[12] A. Tomaradze,[12] P. Zweber,[12] J. Ernst,[13] H. Severini,[14] D. M. Asner,[15] S. A. Dytman,[15] W. Love,[15] S. Mehrabyan,[15] J. A. Mueller,[15] V. Savinov,[15] Z. Li,[16] A. Lopez,[16] H. Mendez,[16] J. Ramirez,[16] G. S. Huang,[17] D. H. Miller,[17] V. Pavlunin,[17] B. Sanghi,[17] I. P. J. Shipsey,[17] G. S. Adams,[18] M. Cravey,[18] J. P. Cummings,[18] I. Danko,[18] J. Napolitano,[18] Q. He,[19] H. Muramatsu,[19] C. S. Park,[19] E. H. Thorndike,[19] T. E. Coan,[20] Y. S. Gao,[20] F. Liu,[20] M. Artuso,[21] C. Boulahouache,[21] S. Blusk,[21] J. Butt,[21] O. Dorjkhaidav,[21] J. Li,[21] N. Menaa,[21] R. Mountain,[21] R. Nandakumar,[21] K. Randrianarivony,[21] R. Redjimi,[21] R. Sia,[21] T. Skwarnicki,[21] S. Stone,[21] J. C. Wang,[21] K. Zhang,[21] and S. E. Csorna[22]

(CLEO Collaboration)

[1]*Wayne State University, Detroit, Michigan 48202*
[2]*Carnegie Mellon University, Pittsburgh, Pennsylvania 15213*
[3]*Enrico Fermi Institute, University of Chicago, Chicago, Illinois 60637*
[4]*Cornell University, Ithaca, New York 14853*
[5]*University of Florida, Gainesville, Florida 32611*
[6]*George Mason University, Fairfax, Virginia 22030*
[7]*University of Illinois, Urbana-Champaign, Illinois 61801*
[8]*Carleton University, Ottawa, Ontario, Canada K1S 5B6*
and the Institute of Particle Physics, Canada
[9]*University of Kansas, Lawrence, Kansas 66045*
[10]*Luther College, Decorah, Iowa 52101*
[11]*University of Minnesota, Minneapolis, Minnesota 55455*
[12]*Northwestern University, Evanston, Illinois 60208*
[13]*State University of New York at Albany, Albany, New York 12222*
[14]*University of Oklahoma, Norman, Oklahoma 73019*

[15]*University of Pittsburgh, Pittsburgh, Pennsylvania 15260*
[16]*University of Puerto Rico, Mayaguez, Puerto Rico 00681*
[17]*Purdue University, West Lafayette, Indiana 47907*
[18]*Rensselaer Polytechnic Institute, Troy, New York 12180*
[19]*University of Rochester, Rochester, New York 14627*
[20]*Southern Methodist University, Dallas, Texas 75275*
[21]*Syracuse University, Syracuse, New York 13244*
[22]*Vanderbilt University, Nashville, Tennessee 37235*
(Dated: Jun 12, 2005)

Abstract

We extract a relatively precise value for the decay constant of the D^+ meson by measuring $\mathcal{B}(D^+ \to \mu^+\nu_\mu) = (4.45 \pm 0.67^{+0.29}_{-0.36}) \times 10^{-4}$ using 280 pb^{-1} of data taken on the $\psi(3770)$ resonance with the CLEO-c detector. We find $f_{D^+} = (223 \pm 16^{+7}_{-9})$ MeV . We also set a 90% confidence upper limit on $\mathcal{B}(D^+ \to e^+\nu) < 2.4 \times 10^{-5}$.

*Submitted to the XXII International Symposium on Lepton and Photon Interactions at High Energies, June 30-July 5, 2005, Uppsala, Sweden

I. INTRODUCTION

Measuring purely leptonic decays of heavy mesons allows the determination of meson decay constants, which connect measured quantities, such as the $B\bar{B}$ mixing ratio, to CKM matrix elements. Currently, it is not possible to determine f_B experimentally from leptonic B decays, so theoretical calculations of f_B must be used. The most promising of these calculations involves lattice QCD [1–4], though there are other methods [5–9].

Measurements of pseudoscalar decay constants such as f_{D^+} provide checks on these calculations and help discriminate among different models.

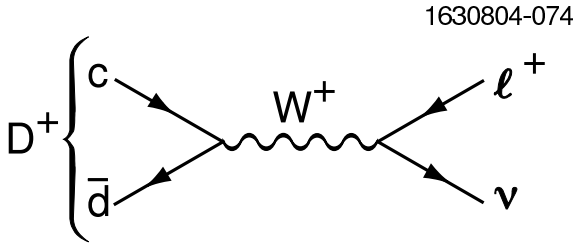

FIG. 1: The decay diagram for $D^+ \to \mu^+\nu$.

The decay diagram for $D^+ \to \mu^+\nu$ is shown in Fig. 1. The decay rate is given by [10]

$$\Gamma(D^+ \to \ell^+\nu) = \frac{G_F^2}{8\pi} f_{D^+}^2 m_\ell^2 M_{D^+} \left(1 - \frac{m_\ell^2}{M_{D^+}^2}\right)^2 |V_{cd}|^2 \quad , \tag{1}$$

where M_{D^+} is the D^+ mass, m_ℓ is the mass of the final state lepton, V_{cd} is a CKM matrix element equal to 0.225 [11], and G_F is the Fermi coupling constant. Various theoretical predictions of f_{D^+} range from 190 MeV to 350 MeV [1–9]. Because of helicity suppression, the electron mode $D^+ \to e^+\nu$ has a very small rate in the Standard Model [12]. The relative widths are $2.65 : 1 : 2.3 \times 10^{-5}$ for the $\tau^+\nu$, $\mu^+\nu$ and $e^+\nu$ final states, respectively. Unfortunately the mode with the largest branching fraction, $\tau^+\nu$, has at least two neutrinos in the final state and is difficult to detect.

The CLEO-c detector is equipped to measure the momenta and direction of charged particles, identify charged hadrons, detect photons, and determine with good precision their directions and energies. It has been described in more detail previously [13], [14], [15], [16].

II. DATA SAMPLE AND SIGNAL SELECTION

In this study we use 280 pb^{-1} of CLEO-c data produced in e^+e^- collisions and recorded at the ψ'' resonance (3.770 GeV). This work contains our previous sample as a subset and supercedes our initial efforts [16]. At this energy, the events consist of a mixture of pure D^+D^-, $D^o\overline{D}^o$, three-flavor continuum and $\gamma\psi'$ events. There may also be small amounts of $\tau^+\tau^-$ pairs and two-photon events.

We examine all the recorded events and retain those containing at least one charged D candidate in the modes listed in Table I. We use this sample to look for cases where we have only a single muon candidate whose four-momentum is consistent with a two-body D

decay into a muon and a neutrino and no other charged tracks or excess neutral energy are present. Track selection, particle identification, π^o, K_S and muon selection cuts are identical to those described in reference [16].

III. RECONSTRUCTION OF CHARGED D TAGGING MODES

Tagging modes are fully reconstructed by first evaluating the difference in the energy, ΔE, of the decay products with the beam energy. We require the absolute value of this difference to contain 98.8% of the signal events, i. e. to be within ∼2.5 times the r.m.s width of the peak value. The r.m.s. widths vary from ∼7 MeV in the $K^+K^-\pi^-$ mode to ∼14 MeV in the $K^+\pi^-\pi^-\pi^o$ mode. For the selected events we then view the reconstructed D^- beam-constrained mass defined as

$$m_{BC} = \sqrt{E^2_{beam} - (\sum_i \overrightarrow{p}_i)^2}, \tag{2}$$

where i runs over all the final state particles. The beam-constrained mass has better resolution then merely calculating the invariant mass of the decay products since the beam has a small energy spread. Besides using D^- tags and searching for $D^+ \to \mu^+\nu$, we also use the charge-conjugate D^+ tags and search for $D^- \to \mu^-\overline{\nu}_\mu$; in the rest of this paper we will not mention the charge-conjugate modes explicitly, but they are always used.

The m_{BC} distributions for all D^- tagging modes considered in this data sample are shown in Fig. 2 and listed in Table I along with the numbers of signal events and background events within the signal region defined as containing 98.8% of the signal events with m_{BC} below the peak and 95.5% of the signal events above the peak. The event numbers are determined from fits of the m_{BC} distributions to a signal function plus a background shape. For the background we fit with a shape function analogous to one first used by the ARGUS collaboration [22] which has approximately the correct threshold behavior at large m_{BC}; to use this function, we first fit it to the data selected by using ΔE sidebands, mode by mode, defined as $5\sigma < |\Delta E| < 7.5\sigma$, where σ is the r.m.s. width of the ΔE distribution, to fix the shape parameters in each mode allowing the normalization to float. For the signal we use a lineshape similar to that used by for extracting photon signals from electromagnetic calorimeters because of the tail towards high mass caused by initial state radiation [17]. The functional form is

$$f(m_{BC}|m_D,\sigma_{m_{BC}},\alpha,n) = \begin{cases} A\cdot\exp\left[-\frac{1}{2}\left(\frac{m_{BC}-m_D}{\sigma_{m_{BC}}}\right)^2\right] & \text{for } m_{BC} < m_D - \alpha\cdot\sigma_{m_{BC}} \\ A\cdot\frac{\left(\frac{n}{\alpha}\right)^n e^{-\frac{1}{2}\alpha^2}}{\left(\frac{m_{BC}-m_D}{\sigma_{m_{BC}}}+\frac{n}{\alpha}-\alpha\right)^n} & \text{for } m_{BC} > m_D - \alpha\cdot\sigma_{m_{BC}} \\ \text{here } A^{-1} \equiv \sigma_{m_{BC}}\cdot\left[\frac{n}{\alpha}\cdot\frac{1}{n-1}e^{-\frac{1}{2}\alpha^2} + \sqrt{\frac{\pi}{2}}\left(1+\text{erf}\left(\frac{\alpha}{\sqrt{2}}\right)\right)\right] & \end{cases} \tag{3}$$

Here m_{BC} is the measured mass, m_D is the "true" (or most likely) mass and $\sigma_{m_{BC}}$ is the mass resolution.

We use a total of 158,354±496±475 single tag events for further analysis. The systematic error on this number is given by varying the background function and is estimated at 0.3%.

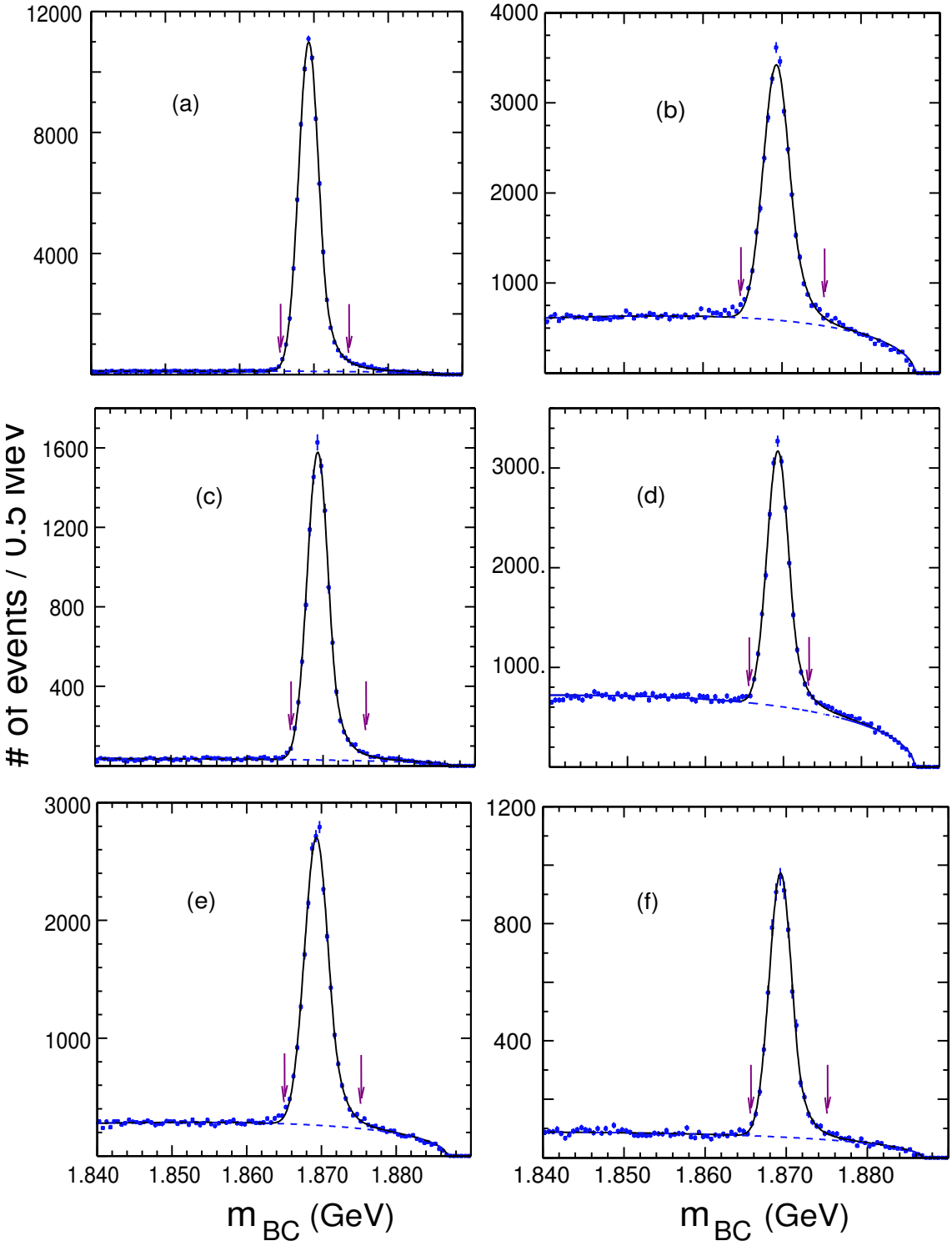

FIG. 2: Beam-constrained mass distributions for different fully reconstructed D^- decay candidates in the final states: (a) $K^+\pi^-\pi^-$, (b) $K^+\pi^-\pi^-\pi^0$, (c) $K_S\pi^-$, (d) $K_S\pi^-\pi^-\pi^+$, (e) $K_S\pi^-\pi^0$ and (f) $K^+K^-\pi^-$. The solid curves show the sum of signal and background functions. The dashed curves indicate the background fits. Events between the arrows are selected for further analysis.

Mode	Signal	Background
$K^+\pi^-\pi^-$	77387 ± 281	1868
$K^+\pi^-\pi^-\pi^o$	24850 ± 214	12825
$K_S\pi^-$	11162 ± 136	514
$K_S\pi^-\pi^-\pi^+$	18176 ± 255	8976
$K_S\pi^-\pi^o$	20244 ± 170	5223
$K^+K^-\pi^-$	6535 ± 95	1271
Sum	158354 ± 496	30677

TABLE I: Tagging modes and numbers of signal and background events determined from the fits shown in Fig. 2.

IV. $D^+ \to \mu^+\nu_\mu$ SELECTION CRITERIA

Using our sample of D^- event candidates we search for events with a single additional charged track presumed to be a μ^+. Then we infer the existence of the neutrino by requiring a measured value near zero (the neutrino mass) of the missing mass squared (MM^2) defined as

$$\mathrm{MM}^2 = (E_{beam} - E_{\mu^+})^2 - \left(-\overrightarrow{p}_{D^-} - \overrightarrow{p}_{\mu^+}\right)^2, \tag{4}$$

where $\overrightarrow{p}_{D^-}$ is the three-momentum of the fully reconstructed D^-.

We need to restrict the sample to candidate $\mu^+\nu_\mu$ events resulting from the other D. Thus we wish to exclude events with more than one additional track with opposite charged to the tagged D, which we take to be the muon candidate, or with extra neutral energy. Our criteria is to veto events with charged tracks arising from the event vertex or having a maximum neutral energy cluster, consistent with being a photon, of more than 250 MeV. These cuts are highly effective in reducing backgrounds especially from $D^+ \to \pi^+\pi^o$ decays. We need, however, to evaluate the efficiency of these cuts.

It is possible, in fact even likely, that the decay products of the tagging D^- interact in the detector material, mostly the EM calorimeter and spray tracks and neutral energy back into the rest of the detector. We evaluate the size of these contributions by using fully reconstructed D^+D^- events. (The method is different here than in our original publication, though the results are consistent.)

Although we do not expect more than a few percent background in these event samples, we do not want to incur a systematic error due to this potential source. Therefore we perform a full five constraint kinematic fit to the event samples; the constraints are that the total energy sum to twice the beam energy, that the total three momentum be zero and that the invariant masses of the two D candidates be equal. We do not require them to equal the known D^+ mass. The result of this fit is a common D candidate mass and a χ^2. Restricting our samples to low χ^2 virtually eliminates all backgrounds at the expenses of some signal. The numbers of these events in the decay modes we use are listed in Table II.

To first order the fully reconstructed $D^+D^- \to K^+\pi^-\pi^-$, $K^-\pi^+\pi^+$ can be considered the superposition of two single tag $D^+ \to \mu^+\nu$ candidate events where the single tag is $K^-\pi^+\pi^+$. Our procedure is to evaluate our cut efficiency in this sample and then divide by two. This gives us the efficiency for the $D^- \to K^-\pi^+\pi^+$ tag sample. We then combine the large and

Mode 1	Mode 2	# of events	$\#(E_{\gamma>250\ \mathrm{MeV}})$	$\epsilon(\%)$ of Mode 1
$K^+\pi^-\pi^-$	$K^-\pi^+\pi^+$	861	82	95.2±0.5
$K^+\pi^-\pi^-\pi^o$	$K^-\pi^+\pi^+$	468	25	99.4±1.2
$K_S\pi^-$	$K^-\pi^+\pi^+$	242	24	94.8±2.0
$K_S\pi^-\pi^-\pi^+$	$K^-\pi^+\pi^+$	406	28	97.9±1.4
$K_S\pi^-\pi^o$	$K^-\pi^+\pi^+$	524	42	96.7±1.3
$K^+K^-\pi^-$	$K^-\pi^+\pi^+$	143	17	92.9±2.8
Weighted Average				96.3±0.4

TABLE II: Numbers of D^+D^- events and the efficiency for the first mode when an extra photon > 250 MeV is also required.

precise $K^-\pi^+\pi^+$ with each of the other tags in turn. This method ensures that the number of interactions of particles with material and their consequences is the same as in the tag sample used for the $\mu^+\nu$ analysis.

Extra tracks do appear in these D^+D^- events. None of these tracks, however, approach the main event vertex. Requiring that good tracks are within 5 cm along the beam and 5 mm perpendicular to the beam does not include any additional tracks from interactions in the material. We also reject D^- tags with additional $K_S \to \pi^+\pi^-$ candidates.

We accept only as extra showers those that do not match a charged track within a connected region. A connected region is a group of adjacent crystals with energy depositions which are nearest neighbors. This suppresses hadronic shower fragments which would otherwise show up as unmatched showers. Hadronic interactions and very energetic π^o's tend to produce one connected region with many clusters.

The results are listed in Table II. The numbers of events listed are those with a χ^2 cut applied. The efficiency for accepting the double tag event requiring that there not be any photons above 250 MeV is given along with the derived efficiency for each mode. A weighted average over all our tag modes gives an efficiency of (96.3±0.4±0.4)% quite consistent with the (93.5±0.9±4.0)% we previously found using a $D^o\overline{D}^o$ tag sample. Now, however, the systematic error arises only from the consideration that we have analyzed a situation corresponding to two overlaping tags rather than one tag plus a muon, and is much smaller.

The muon candidate is required to be within the barrel region of the detector $|\cos\theta| < 0.81$, and deposit less than 300 MeV of energy in the calorimeter, characteristic of a minimum ionizing particle.

The MM^2 from Monte Carlo simulation is shown in Fig. 3 for the $K^-\pi^+\pi^+$ tag mode. The signal is fit to a sum of two Gaussians with the wider Gaussian having about 30% of the area independent of tagging mode. The resolution (σ) is defined as

$$\sigma = f_1\sigma_1 + (1 - f_1)\sigma_2, \tag{5}$$

where σ_1 and σ_2 are the individual widths of the two Gaussians and f_1 is the fractional area of the first Gaussian. The resolution is 0.0235±0.0004 GeV^2 consistent among all the tagging decay modes.

We check our simulations by using the $D^+ \to K_S\pi^+$ decay. Here we choose events with the same requirements as used to search for $\mu^+\nu$ but require one additional found K_S. The

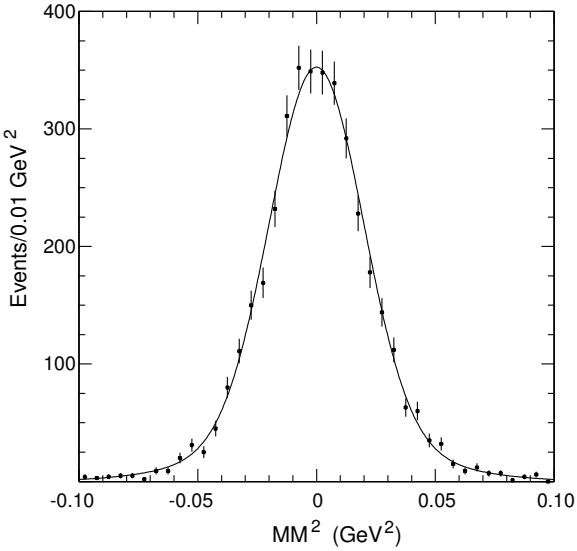

FIG. 3: Monte Carlo simulation of the MM^2 distributions for $D^+ \to \mu^+\nu_\mu$ events using the $K^-\pi^+\pi^+$ tag. The fit is to two Gaussians centered at zero where the second Gaussian constitutes around 30% of area.

MM^2 distribution for this final state is shown in Fig. 4 and peaks as expected at the K_S mass-squared of 0.25 GeV^2. The resolution is measured to be 0.0233±0.0009 GeV^2 from the double Gaussian fit, consistent with the Monte Carlo estimate of 0.0222±0.0005 GeV^2.

The MM^2 distributions for our tagged events requiring no extra charged tracks besides the muon candidate and showers above 250 MeV as described above is shown in Fig. 5. We see a signal near zero containing 50 events within an interval, −0.050 GeV^2 to +0.050 GeV^2, approximately $\pm 2\sigma$. This signal is mostly due to the $D^+ \to \mu^+\nu_\mu$ mode we are seeking. The large peak centered near 0.25 GeV^2 is from the decay $D^+ \to \overline{K}^o\pi^+$ that is far from our signal region and is expected since many K_L would escape our detector.

V. BACKGROUND EVALUATION

There are several background sources we need to evaluate. These include background from other D^+ modes, background from misidentified $D^o\overline{D}^o$ events and continuum background including that from $e^+e^- \to \gamma\psi'$, termed "radiative return." Hadronic sources need to be considered because the requirement of the muon depositing <300 MeV in the calorimeter, while about 99% efficient on muons, rejects only about 40% of pions as determined from the $D^o\overline{D}^o$ event sample where the pion from the $K^\pm\pi^\mp$ mode was examined.

There are a few D^+ decay modes that could mimic the signal. These are listed in Table III along with the background estimate we obtained by Monte Carlo generation and reconstruction of each specific mode. The branching ratios are from the Particle Data Group except for the $\pi^+\pi^o$ mode where a separate CLEO analysis gives a somewhat lower value [18]. This mode is the most difficult to reject because the MM^2 peaks very close to zero, at 0.018 GeV^2, well within our resolution of 0.025 GeV^2. While we have insisted that the muon candidate be well within our acceptance, it is possible for the photons from the π^o decay to inadver-

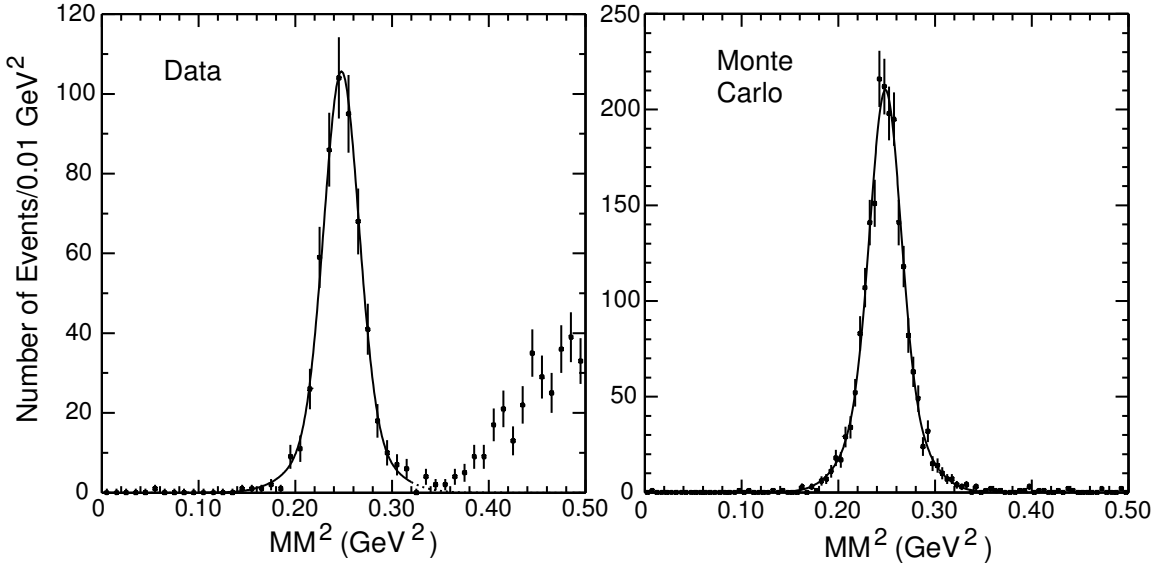

FIG. 4: MM^2 distribution for the decay $D^+ \to K_S\pi^+$ from data and signal Monte-Carlo simulation

tently be matched to the tracks from the tagging D^- or be missed. We note that at least one photon from the $\pi^+\pi^o$ mode exceeds our 250 MeV calorimeter energy requirement and should in most cases cause such a decay to be vetoed.

The $\overline{K}^o\pi^+$ mode gives a large peak in the MM^2 spectrum near 0.25 GeV^2. While it is many r.m.s. widths from our signal region, we need to evaluate the effects of the tail of the distribution. A simulation shows only a very small contamination of only 0.44±0.22 events. We also measure this background rate directly. We use the double tag D^o events where one D decays into $K^\mp\pi^\pm$. Here we gather a sample of single tags, either $K^-\pi^+\pi^+\pi^-$, $K^-\pi^+\pi^o$ or $K^-\pi^+$ and look for events with only two oppositely signed tracks where the ring imaging Cherenkov system identifies one as a kaon and other as a pion. Then we ignore the kaon. The MM^2 of distribution is shown on Fig. 6. There is only one event in the signal region, corresponding to a background of 0.44±0.44 events in our sample.

We have simulated backgrounds from $D^+ \to \tau^+\nu$. Out of 10,000 simulated events with D^- tags, we found background only when $\tau^+ \to \pi^+\nu$. Because of the small D^+-τ^+ mass difference, the τ^+ is almost at rest in the laboratory frame and thus the π^+ has relatively large momentum causing the MM^2 distribution to populate only the low MM^2 region, even in this case with two missing neutrinos.

We have also checked the possibility of other D^+D^- decay modes producing background with an equivalent 1.7 fb^{-1} sample; we find no additional events. $D^o\overline{D}^o$ and continuum backgrounds are also evaluated by analyzing Monte Carlo samples corresponding to 0.54 fb^{-1}. To normalize our Monte Carlo events to our data sample we used $\sigma_{D^o\overline{D}^o} = 3.5$ nb and $\sigma_{continuum} = 14.5$ nb [19]. We found no events in any of these samples.

Our total background is 2.92±0.50 events. The backgrounds from other D^+, D^o and continuum sources are limited to less than 0.4, 0.4 and 1.2 events at 90% confidence level, respectively. To account for possible backgrounds from these sources we add them as 32% confidence level (1σ) values in quadrature for a positive error and therefore add an additional $^{+0.8}_{-0}$ event systematic error. Systematic errors on the $\pi^+\pi^o$ and $\tau\nu$ backgrounds arise from errors in the branching fraction and are already included in the estimate.

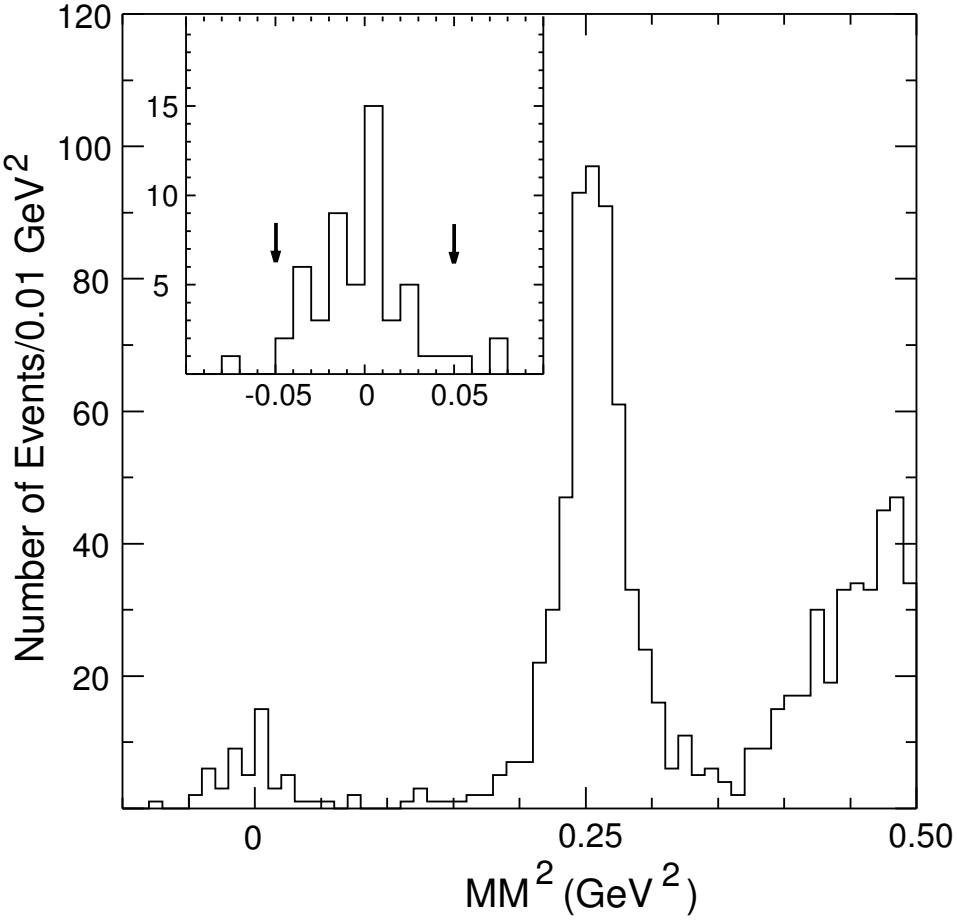

FIG. 5: MM^2 using D^- tags and one additional opposite sign charged track and no extra energetic showers (see text). The insert shows the signal region for $D^+ \to \mu^+\nu$ enlarged; the defined signal region is shown between the two arrows.

VI. BRANCHING RATIO AND DECAY CONSTANT

We have $47.1\pm7.1^{+2.9}_{-3.7}$ $\mu^+\nu$ signal events after subtracting background. In our sample of 158,354 signal tags. The detection efficiency for the single muon of 69.4.c% includes the selection on MM^2 within $\pm2\sigma$ limits, the tracking, the particle identification and probability of the crystal energy being less than 300 MeV. It does not include the 96.3% efficiency of not having another unmatched shower in the event with energy greater than 250 MeV. This efficiency is determined from the data presented in Table II. The systematic errors on the branching ratio are listed in Table IV.

Our result for the branching fraction is

$$\mathcal{B}(D^+ \to \mu^+\nu_\mu) = (4.45 \pm 0.67^{+0.29}_{-0.36}) \times 10^{-4} \ . \tag{6}$$

The decay constant f_{D^+} is then obtained from Eq. (1) using 1.040 ps as the D^+ lifetime and 0.225 as $|V_{cd}|$ [11]. Our final result is

$$f_{D^+} = (223 \pm 16^{+7}_{-9}) \text{ MeV} \ . \tag{7}$$

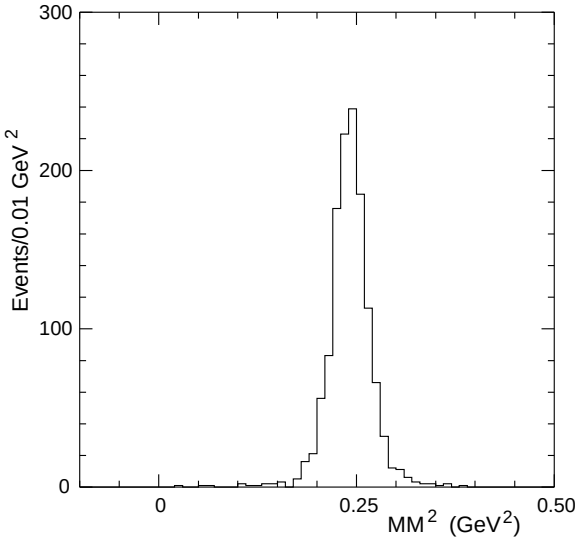

FIG. 6: The MM^2 from events with a single D^o tag and the other D decaying into two tracks, most likely $D^o \to K^-\pi^+$, where the kaon is ignored.

Mode	$\mathcal{B}$ (%)	# of events
$\pi^+\pi^o$	0.13±0.02	1.40±0.18
$\overline{K}^o\pi^+$	2.77±0.18	0.44±0.44
$\tau^+\nu$	2.65× $\mathcal{B}(D^+ \to \mu^+\nu)$	1.08±0.15
Other D^+ modes		0
D^o modes		0
Continuum		0
Sum		2.92±0.50

TABLE III: Backgrounds from all sources

VII. SEARCH FOR $D^+ \to e^+\nu_e$

We use the same tag sample. We identify the electron using a match between the momentum measurement in the tracking system and the energy deposited in the CsI calorimeter as well as insuring that the shape of the energy distribution among the crystals is consistent with that expected for an electromagnetic shower. Other cuts remain the same. We don't find any candidates allowing us to set a limit

$$\mathcal{B}(D^+ \to e^+\nu_e) < 2.4 \times 10^{-5} \ . \tag{8}$$

VIII. CONCLUSIONS

We significantly improved our previous result and now report on five times our previous data. The errors, both statistical and systematic have been reduced by more than a factor of two.

	Systematic errors (%)
MC statistics	0.4
Track finding	0.7
PID cut	1.0
MM^2 width	1.0
Minimum ionization cut	1.0
Number of tags	0.3
Extra showers cut	0.6
Total	2.0

TABLE IV: Systematic errors on the $D^+ \to \mu^+\nu_\mu$ branching ratio.

The branching fraction is

$$\mathcal{B}(D^+ \to \mu^+\nu_\mu) = (4.45 \pm 0.67^{+0.29}_{-0.36}) \times 10^{-4}, \tag{9}$$

and the decay constant is

$$f_{D^+} = (223 \pm 16^{+7}_{-9}) \text{ MeV} . \tag{10}$$

Our results are consistent with our previous result [16] as well other attempts to measure the decay constant from Mark III [20] and BES [23].

Our result for f_{D^+}, at the current level of precision, is consistent with predictions of lattice QCD and models listed in Table V.

Model	f_{D^+} (MeV)	$f_{D_s^+}/f_{D^+}$
Lattice QCD (Fermilab and MILC) [2]	$225^{+11}_{-13} \pm 21$	$1.17 \pm 0.06 \pm 0.06$
Quenched Lattice QCD (UKQCD) [3]	$210 \pm 10^{+17}_{-16}$	$1.13 \pm 0.02^{+0.04}_{-0.02}$
Quenched Lattice QCD [4]	$211 \pm 14^{+0}_{-12}$	1.10 ± 0.02
QCD Spectral Sum Rules [6]	203 ± 20	1.15 ± 0.04
QCD Sum Rules [7]	195 ± 20	
Relativistic Quark Model [8]	243 ± 25	1.10
Potential Model [5]	238	1.01
Isospin Mass Splittings [9]	262 ± 29	

TABLE V: Theoretical predictions of f_{D^+} and $f_{D_s^+}/f_{D^+}$

The models generally predict $f_{D_s^+}$ to be 10-15% larger than f_{D^+}. CLEO previously measured $f_{D_s^+}$ as $(280 \pm 19 \pm 28 \pm 34)$ MeV [24], and we are consistent with these predictions as well.

Some non-standard models predict significant rates for the helicity suppress decay $D^+ \to e^+\nu$ [25]. Our upper limit of 2.4×10^{-5} at 90% c.l. restricts these models.

IX. ACKNOWLEDGMENTS

We gratefully acknowledge the effort of the CESR staff in providing us with excellent luminosity and running conditions. This work was supported by the National Science Foundation and the U.S. Department of Energy.

---

[1] C. Davies *et al.*, Phys. Rev. Lett. **92**, 022001 (2004) [hep-lat/0304004]; C. Davies, "Lattice QCD," in Heavy Flavour Physics, Scottish Graduate Textbook Series, Institute of Physics 2002, eds. C. T. H. Davies and S. M. Playfer [hep-ph/025181] and references therein; A. Kronfeld, "Heavy Quarks and Lattice QCD," [hep-lat/0310063] and references therein.

[2] J. Simone *et al.* (MILC), "Leptonic decay constants f_{D_s} and f_D in three flavor lattice QCD," (2004) [hep-lat/0410030].

[3] L. Lellouch and C.-J. Lin (UKQCD), Phys. Rev. **D64**, 094501 (2001).

[4] D. Becirevic *et al.*, Phys. Rev. **D60**, 074501(1999) [hep-lat/9811003].

[5] Z. G. Wang *et al.*, "Decay Constants of the Pseudoscalar Mesons in the framework of the Coupled Schwinger-Dyson Equation and Bethe-Salpeter Equation," [hep-ph/0403259] (2004); L. Salcedo *et al.*, Braz. J. Phys. **34**, 297 (2004) [hep-ph/0311008].

[6] S. Narison, "Light and Heavy Quark Masses, Flavour Breaking of Chiral Condensates, Meson Weak Leptonic Decay Constants in QCD," [hep-ph/0202200] (2002).

[7] A. Penin and M. Steinhauser, Phys. Rev. **D65**, 054006 (2002).

[8] D. Ebert *et al.*, Mod. Phys. Lett. **A17**, 803 (2002).

[9] J. Amundson *et al.*, Phys. Rev. **D47** 3059 (1993) [hep-ph/9207235].

[10] J. L. Rosner, in **Particles and Fields 3**, Proceed. of the 1988 Banff Summer Inst., Banff, Alberta, Canada, ed. by A. N. Kamal and F. C. Khanna, World Scientific, Singapore, 1989, 395.

[11] We assume that $|V_{cd}|$ equals $|V_{us}|$ and take the value from the new KTeV result, T. Alexopoulos *et al.* Phys. Rev. Lett. **93**, 181802 (2004) [hep-ex/0406001].

[12] Non-Standard Models predict different ratios; see for example A. G. Akeroyd and S. Recksiegel, Phys. Lett. B **554**, 38 (2003) [hep-ph/0210376].

[13] D. Peterson *et al.*, Nucl. Instrum. and Meth. **A478**, 142 (2002).

[14] M. Artuso *et al.*, Nucl. Instrum. and Meth. **A502**, 91 (2003).

[15] Y. Kubota *et al.* (CLEO), Nucl. Instrum. and Meth. **A320**, 66 (1992).

[16] G. Bonvicini *et al.* CLEO, Phys. Rev. **D70**, 112004 2004 [hep-ex/0411050].

[17] T. Skwarnicki, "A Study of the Radiative Cascade Transitions Between the Upsilon-Prime and Upsilon Resonances," DESY F31-86-02 (thesis, unpublished) (1986).

[18] K. Arms *et al.* (CLEO), Phys. Rev. **D69**, 071102 (2004) [hep-ex/0309065].

[19] CLEO Collaboration, Q. He *et al.*., CLNS-05-1914, hep-ex/0504003, submitted to PRL.

[20] J. Adler *et al.* (Mark III), Phys. Rev. Lett. **60** 1375 (1988); erratum-ibid, **63**, 1658 (1989).

[21] J. Z. Bai *et al.* (BES), Phys. Lett. B **429**, 188 (1998).

[22] The function is $f(m_{BC}) = A(m_{BC}+B)\sqrt{1-\left(\frac{m_{BC}+B}{C}\right)^2}\, e^{D\left(1-\left[\frac{m_{BC}+B}{C}\right]^2\right)}$. Here A is the overall normalization and B, C and D are parameters that govern the shape. See H. Albrecht *et al.* (ARGUS), Phys. Lett. B **229**, 304(1989).

[23] M. Ablikim *et al.*, "Direct Measurement of the Pseudoscalar Decay Constant f_{D^+}," [hep-ex/0410050].
[24] M. Chadha *et al.* (CLEO), Phys. Rev. **D58**, 032002 (1998) [hep-ex/9712014].
[25] A.G. Akeroyd and S.Recksiegel, Phys. Lett. **B549**, 314 (2002) [hep-ph/0210276] and references contained therein.